3-2-2021

In Situ Preconcentration and Quantification of Cu^{2+} via Chelating Polymer-Wrapped Multiwalled Carbon Nanotubes

P. U.Ashvin Iresh Fernando

Erik Alberts

Matthew W. Glasscott

Anton Netchaev

Jason D. Ray

See next page for additional authors

Recommended Citation

Fernando, PU Ashvin Iresh, Erik Alberts, Matthew W. Glasscott, Anton Netchaev, Jason D. Ray, Keith Conley, Rishi Patel et al. "In Situ Preconcentration and Quantification of Cu2+ via Chelating Polymer-Wrapped Multiwalled Carbon Nanotubes." ACS omega 6, no. 8 (2021): 5158-5165.

ACS OMEGA

http://pubs.acs.org/journal/acsodf

Article

In Situ Preconcentration and Quantification of Cu^{2+} via Chelating Polymer-Wrapped Multiwalled Carbon Nanotubes

P. U. Ashvin Iresh Fernando, Erik Alberts, Matthew W. Glasscott, Anton Netchaev, Jason D. Ray, Keith Conley, Rishi Patel, Jonathan Fury, David Henderson, Lee C. Moores, and Gilbert K. Kosgei*

Cite This: *ACS Omega* 2021, 6, 5158−5165

Read Online

ACCESS | Metrics & More | Article Recommendations | Supporting Information

ABSTRACT: Trace analysis of heavy metals in complex, environmentally relevant matrices remains a significant challenge for electrochemical sensors employing stripping voltammetry-based detection schemes. We present an alternative method capable of selectively preconcentrating Cu^{2+} ions at the electrode surface using chelating polymer-wrapped multiwalled carbon nanotubes (MWCNTs). An electrochemical sensor consisting of poly-4-vinyl pyridine (P4VP)-wrapped MWCNTs anchored to a poly(ethylene terephthalate) (PET)-modified gold electrode (r = 1.5 mm) was designed, produced, and evaluated. The P4VP is shown to form a strong association with Cu^{2+} ions, permitting preconcentration adjacent to the electrode surface for interrogation via cyclic voltammetry. The sensor exhibited a detection limit of 0.5 ppm with a linear range of 1.1−13.8 ppm (16.6−216 μM) and a relative standard deviation (RSD) of 4.9% at the Environmental Protection Agency (EPA) limit of 1.3 ppm. Evaluation in tap water, lake water, ocean water, and deionized water rendered similar results, highlighting the generalizability of the presented preconcentration strategy. The advantages of electrochemical analysis paired with polymeric chelation represent an effective platform for the design and deployment of heavy metal sensors for continuous monitoring of natural waters.

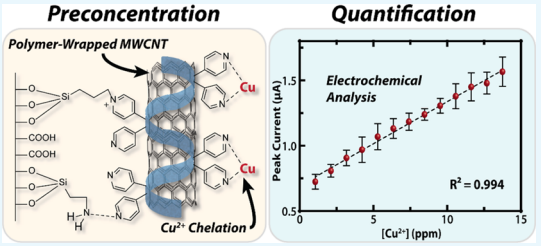

1. INTRODUCTION

The prominence of copper throughout human history may be attributed to its malleability and ductility as a native metal and in alloys, excellent thermal and electrical conductivity, and antimicrobial properties.[1] Due to these versatile physicochemical properties, copper is present in a variety of consumer products including electrical appliances, pesticides, and wood preservatives.[2] Additionally, copper is widely used in processes such as electroplating, azo dye manufacturing, engraving, lithography, petroleum refining, and pyrotechnics.[3] However, the prevalence of anthropogenic copper raises concerns regarding its environmental fate and toxicity. At harmful levels, copper ions may result in multiple human health issues including vomiting, diarrhea, stomach cramps, nausea, liver damage, and other related kidney diseases.[4] Due to these concerns, the United States Environmental Protection Agency (EPA) has set a maximum allowable copper concentration of 1.3 ppm (20 μM) in drinking water.[5]

While a number of detection strategies exist for aqueous copper ions, most require significant instrumental infrastructure and are relatively costly, prohibiting their incorporation into low size, weight, power, and cost (SWaP-C) deployable platforms. Fluorometric assay-based studies are widely used in copper detection. However, these involve multistep synthetic processes, which increase the cost of the sensor and complicate scalability for practical applications.[6−8] Electrochemical analysis via anodic stripping voltammetry (ASV) constitutes a widely investigated detection strategy. These techniques are simple to effectuate and are generally administered in two steps. First, the metal analyte is cathodically deposited at the electrode surface for a set period of time (preconcentration). Second, anodic stripping of the metal is initiated to produce an electrochemical signal proportional to the number of atoms stripped from the surface. Despite extensively documented success in laboratory settings, such sensors are underrepresented in commercial markets. While anodic stripping voltammetry represents a simple preconcentration strategy for multiple metallic species, analysis of the electrochemical signal may be complicated by variations in pH, alloy and amalgam formation, and competing electrochemical reactions such as oxygen reduction. Oxygen interference, normally eliminated in laboratory settings by purging with inert gas, represents a particularly significant consideration for deployable ASV-based sensors due to its presence in virtually all natural waterways. Furthermore, the application of the deposition voltage for extended periods of time may require a substantial power source not amenable to

Received: September 29, 2020
Accepted: November 19, 2020
Published: February 16, 2021

https://dx.doi.org/10.1021/acsomega.0c04776
ACS Omega 2021, 6, 5158−5165

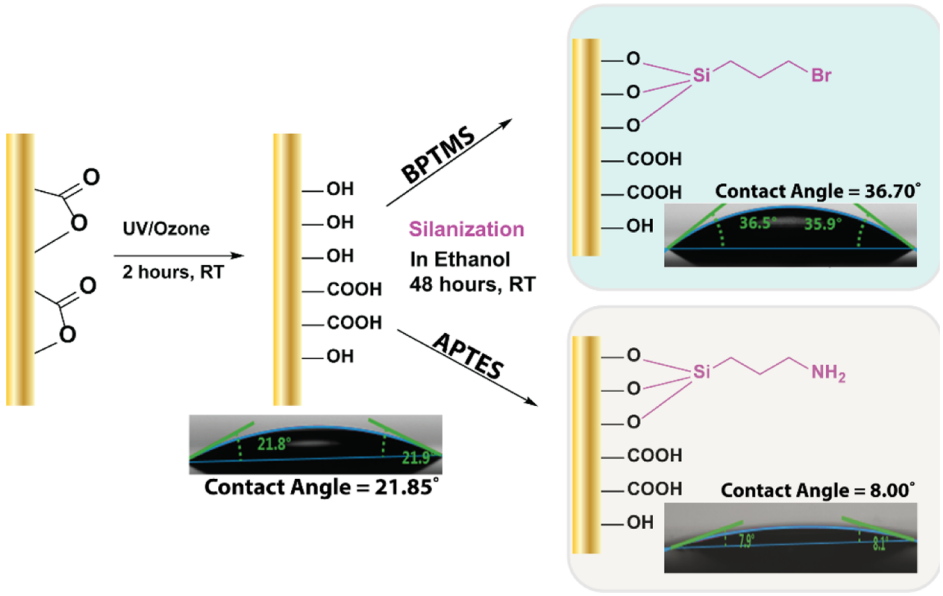

Figure 1. Synthetic steps for the fabrication of sensors with contact angle measurements.

deployable sensors.[9−11] Thus, the generation of robust, low SWaP-C, deployable sensors requires the identification of alternative detection strategies for heavy metal preconcentration and detection in environmentally relevant matrices.

Recently, carbon nanotube (CNT)-based sensors have been used in a variety of applications including environmental toxicant monitoring, the food and agriculture industries, national security, biology, catalysis,[12] and health applications.[13,14] CNTs are versatile, high surface-area structures that may be grafted onto a variety of substrates and have excellent electrical conductivity,[13,15] making them an ideal candidate for electrochemical sensor platforms. Noncovalent modification through polymer wrapping can provide the benefit of attaching functional groups to the CNT while preserving their structure and conductivity[15] and also promote CNT assembly and substrate adherence.[12,16] We hypothesized that these functional groups may be tuned to promote chelation of specific ions in an aqueous matrix, effectively trapping a target analyte adjacent to the electrode surface for subsequent analysis. In this work, we utilized poly-4-vinyl pyridine (P4VP)-wrapped CNTs for the selective preconcentration and quantitation of Cu^{2+} and demonstrated the selectivity of the sensor in various liquid matrices (tap water, lake water, ocean water, deionized water). Importantly, the chelating polymer-wrapped CNTs permit specificity due to the selective binding of P4VP with the copper cation while enhancing sensitivity due to the high surface area and conductivity afforded by CNTs. The sensor infrastructure was extensively characterized using Raman spectroscopy, scanning electron microscopy (SEM), energy-dispersive spectroscopy (EDX), atomic force microscopy (AFM), infrared spectroscopy, and contact angle measurements. Electrochemical interrogation by cyclic voltammetry produced a linear calibration curve between 1.1 and 13.8 ppm (16.6−216 μM), demonstrating the efficiency of the chelating polymer preconcentration strategy for trace analysis. While chelating polymers have been used previously for a myriad of applications (*vide supra*), the unique coupling of P4VP to CNT-modified electrodes for electrochemical sensing has not been previously reported to our knowledge. Thus, the polymer-wrapped MWCNT sensor offers the preconcentration benefits of anodic stripping voltammetry with lower power requirements as well as reduced costs compared to fluorometric methods. The chelating polymer-wrapped MWCNT strategy represents a robust platform for electrochemical sensing with an emphasis on ease of use, cost-efficient production, low power consumption, and trace analysis of heavy metals.

2. RESULTS AND DISCUSSION

Validation of the electrode surface functionalization and sensor performance focused on three major areas: (1) functionalization of the poly(ethylene terephthalate) (PET)-based polymer film, (2) achieving uniform dispersion of polymer-wrapped CNTs and spray coating of CNT dispersions with accuracy on the sensor surfaces, and (3) analysis of sensor performance using electrochemical studies.

2.1. Functionalization of a Polyethylene Terephthalate (PET)-Based Polymer Film. Figure 1 shows an overview of the functionalization procedure. The optimal UV−Ozone treatment time on the PET surface was determined to be 2 h based on contact angle measurements (Figure S1A), where further treatments did not result in greater wettability.[17] UV−Ozone treatment is preferable over other chemical methods such as strong bases, which strip the sputtered gold from the PET substrate; instead, this technique represents a milder reaction condition which resulted in breaking the ester bonds of the PET substrate,[18,19] resulting in the formation of hydroxyl and carboxyl groups facilitating functionalization[20,21] (Figure S1B). In addition to the PET surface, we observed that prolonged exposure of UV−Ozone (>80 min) induces oxidation of the gold surface, resulting in an oxide/hydroxide layer and increased wettability (Figure S2). Previous literature suggest gold oxide formation after more than 1 h of UV−Ozone exposure, yielding a two-component peak in X-ray photoelectron spectroscopy (XPS) indicative of surface hydroxyls and metal oxide layers.[22,23]

Before treatment with UV−Ozone, the PET was smooth and featureless by SEM but became pitted after oxidation (Figure 2a) in agreement with previous studies.[24] Fourier-

https://dx.doi.org/10.1021/acsomega.0c04776
ACS Omega 2021, 6, 5158−5165

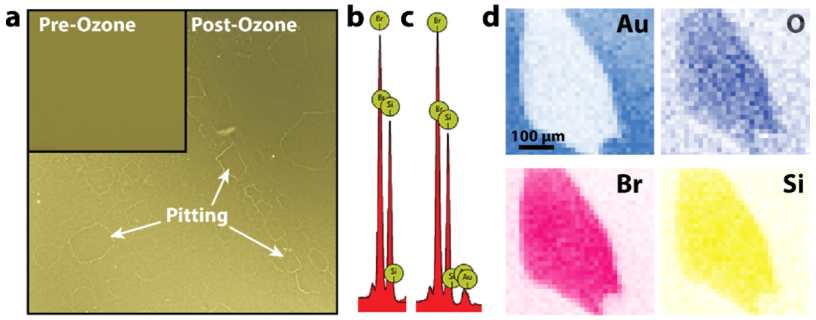

Figure 2. SEM and EDX characterization of sensor surfaces. (a) Pretreated PET surface with functionalization before and after UV/Ozone treatment. Images false-colored to provide contrast. (b) EDX spectra of the PET surface after the BPTMS step. (c) EDX spectra of the gold surface after BPTMS. (d) Elemental mapping profile showing the spatial distribution of functional groups.

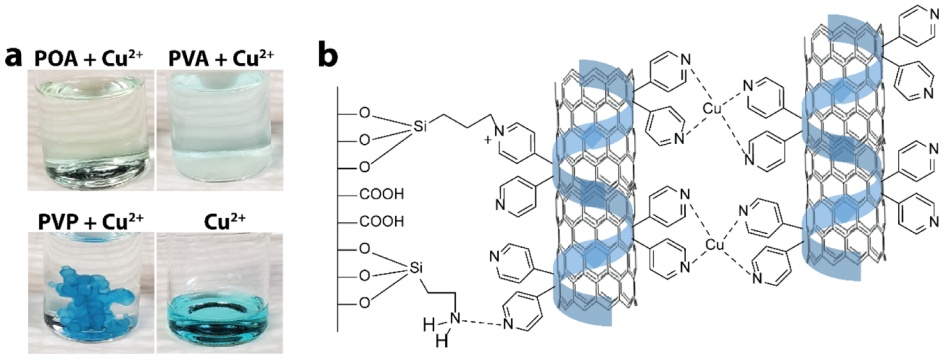

Figure 3. (a) Addition of 3 mL of 1 M $CuSO_4$, 3 mL each to 10 mL of 1 M solution of polymers dissolved in methanol. (b) Representation of surface interactions with the polymer-wrapped CNT and chelation/complexation of copper with pyridyl groups.

transform infrared spectroscopy (FTIR) confirmed the formation of OH groups on the surface with the appearance of a broad absorption band, 3200−3400 cm^{-1}, after treatment (Figure S4). Once the UV−Ozone treatment was completed, the silanization reaction has to be performed with the least amount of air exposure to avoid unwanted oxide layer formations with the newly formed carboxylic acid and hydroxyl groups. Attachment of silanol groups was confirmed with EDX, where the presence of silicon and bromide was observed (Figure 2b). EDX also revealed the gold surface on the working electrode was functionalized during the derivatization of the PET films (Figure 2c,d). This was due to the hydroxyl groups formed during the UV−Ozone step. Attachment of (3-aminopropyl)triethoxysilane (APTES) and (3-bromopropyl)-trimethoxysilane (BPTMS) was further characterized via a contact angle after the silanization reactions. In the case of APTES, the surface became more hydrophilic due to the presence of hydrogen bonding amine groups resulting in a decreased contact angle (21.7−7.9°, Figure S3). The opposite trend was observed in the BPTMS as bromides lowered hydrogen bonding interactions, and contact angle increased from 21.7 to 36.5°.

2.2. Characterizations of Uniform Dispersion of Polymer-Wrapped-CNTs and Spray Coating of CNT Dispersions with Accuracy on Sensor Surfaces. Three different vinylic polymers with similar molecular weights, but different pendent groups, were tested for their ability to serve as the Cu^{2+} ion-selective moiety and CNT dispersant. Poly(vinyl alcohol) (PVA), poly-4-vinyl pyridine (P4VP), and poly(vinyl phenol) (PVO) were chosen due to their ability to form noncovalent interactions with metal ions. Down selection of these polymers was performed by dropwise addition of 1 M $CuSO_4$ solution in DI water to 1 M solution of polymer in methanol shown in Figure 3a. PVA and PVO did not form a precipitate with the addition of copper solution; however, the P4VP solution precipitated instantly when a drop of copper solution was added, indicating complexation, aligning with reported literature.[25−27] Confirmation of the P4VP−Cu complex formation was determined by absorption studies, analysis via inductively coupled plasma atomic emission spectroscopy and mass spectrometry (ICP-MS) (Figure S5). EDX showed sorption of copper to the CNT surfaces after anchoring to the electrode (Figure S6). In Figure 3b, the proposed mechanism of action shows how incoming copper onto the surface of the sensors is trapped in the polymer matrix due to the formation of coordination complexes.

Cationic polymers, such as P4VP, form electrostatic interactions with COO^- groups on MWCNTs, which aids in wrapping.[28,29] Moreover, larger polymers with high molecular weights tend to have a high affinity for wrapping MWCNTs resulting in static stabilization.[30,31] Static stabilization allows the polymer to remain wrapped around the MWCNT after attachment to the sensor surface. Additionally, the pendent pyridyl groups may participate in $\pi-\pi$ stacking interactions, which further stabilizes the MWCNT polymer wrapping process.[32] Polymer wrapping is a noncovalent interaction; therefore, the surface of the nanotubes is kept intact, which preserves the electrical conductivity of the MWCNTs.[33]

The polymer-wrapped MWCNT dispersion was found to be stable up to 5 months in methanol in comparison to MWCNTs alone (Figure S7), indicative of static interactions, as dynamic interactions would have resulted in aggregation.[31,34,35] Methanol was selected as the solvent over other

https://dx.doi.org/10.1021/acsomega.0c04776
ACS Omega 2021, 6, 5158−5165

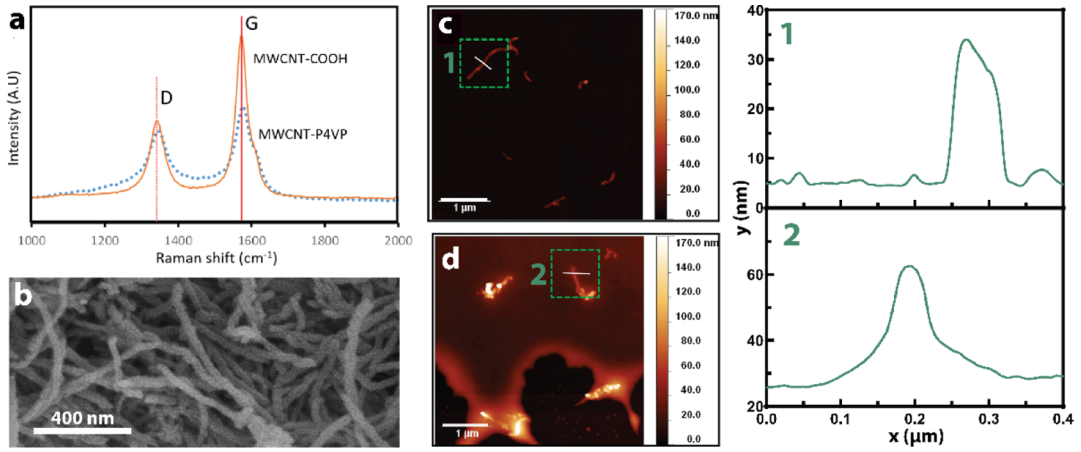

Figure 4. (a) Raman spectra of MWCNT-COOH before (red trace) and after (blue trace) P4VP wrapping. (b) SEM micrograph of P4VP-wrapped MWCNTs. (c) AFM micrograph of raw MWCNT with a representative line-scan profile (1). (d) AFM micrograph of P4VP-MWCNT with a representative line-scan profile (2).

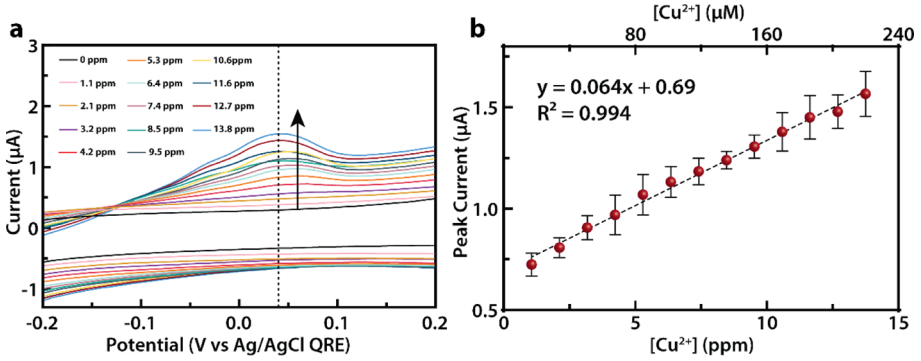

Figure 5. (a) Cyclic voltammograms of copper nitrate $Cu(NO_3)_2$ with increasing concentration of Cu^{2+} ions in solution in 0.1 M $NaNO_3$ using the MWCNT-printed electrodes. (b) Calibration curve obtained from the peak current. Error bars represent the standard deviation from five replicates.

MWCNT dispersing solvents, such as dimethyl sulfoxide (DMSO) and dimethylformamide (DMF), due to its high vapor pressure, allowing for rapid drying necessary in spray printing applications. The Raman spectra in Figure 4a show the characteristic shifts in the sp^2 C−C bonds (G band, ∼1580 cm^{-1}) from 1571 to 1575 cm^{-1}, while the sp^3 defects in graphitic materials (D band, ∼1340 cm^{-1}) remained at 1349 cm^{-1}, indicating MWCNTs were effectively wrapped and dispersed by the P4VP.[36] Additionally, the ratio of intensity in the D band vs the G band (I_D/I_G)[15,36] is 0.66 for COOH-modified MWCNTs and 0.79 for the P4VP-MWCNT dispersion. A significant change in the I_D/I_G value as the P4VP binds to surface noncovalently was not anticipated;[34] however, sp^2 carbons of the P4VP pyridine ring may contribute to the band at 1575 cm^{-1} and the use of sonication in blending the MWCNT/P4VP dispersion may introduce new defects to the MWCNT structure.[35,37] In Figure 4b, P4VP-wrapped MWCNTs appear untangled from each other similar to observations in other literature.[38] Figure 4c,d shows a comparison of representative MWCNT vs polymer-wrapped MWCNTs along with their corresponding height profiles in Figure 4d, showing an increased height and broader peak after wrapping.[39]

The polymer-wrapped MWCNTs were anchored to the electrode surface covalently with BPTMS or through hydrogen bonding with APTES pretreatments.[40] Initially, the dispersion was sprayed on to the sensor using a commercially available manual airbrush. The manual airbrushing resulted in an uneven CNT distribution, which affected the electrochemical response of the sensor. An automated sprayer system (Sono-Tek spray coater, Figure S11) was found to be capable of coating the electrodes with the CNT dispersion accurately, evenly and efficiently with a precision that could not be obtained with a manual airbrush. By controlling the number of layers deposited onto the electrodes and a known concentration of MWCNTs in the dispersion, an aerial density of 0.116 $\mu g/cm^2$ was deposited. Heating the print bed served to initiate covalent or hydrogen bonding between the functionalized sensor surface and the polymer-wrapped CNTs while also evaporating the solvent.

2.3. Sensor Performance Analysis Using Electrochemical Studies. A series of concentration ranges were studied to select the optimal performance of the sensor using cyclic voltammetry. During the electrochemical experiments, equilibration of copper chelation with the P4VP was achieved within 5−10 min across all concentrations. Figure 5a shows the voltammetric response for copper oxidation (0.04 V vs Ag/AgCl QRE). It should be noted that potentials are reported vs a quasi-reference electrode (QRE) due to the nonequilibrium conditions of the screen-printed Ag/AgCl gel reference material. These peaks were observed in the reverse sweep after an initial cathodic sweep to reduce the copper ions. The cathodic peaks are convoluted by the reduction of oxygen and, therefore, unreliable for quantitative analysis. The peak current

https://dx.doi.org/10.1021/acsomega.0c04776
ACS Omega 2021, 6, 5158−5165

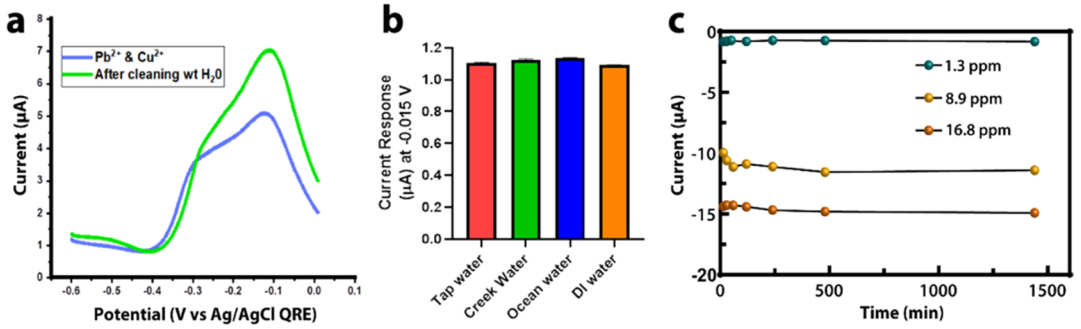

Figure 6. (a) SW voltammogram showing qualitative selectivity toward Cu^{2+} ions by P4VP in the PET electrode platform. (b) Negative current response at −0.015 V for different spiked studies (3 ppm Cu^{2+}). (c) Current responses for the stability test at −0.015 V.

was observed to increase linearly with the concentration between 1.1 and 13.8 ppm (16.6−216 μM), permitting analysis above and below the EPA recommended limit. Typically, 13.8 ppm was chosen as the end point based on the being about 10× the EPA limit (1.3 ppm) and the excellent linearity shown through this range (R^2 = 0.994), showcasing the ability of the polymer-wrapped MWCNT sensor to quantify copper above and below regulatory limits. The individual concentration points were calculated with regard to the volume of a stock Cu^{2+} solution introduced to maximize precision. Furthermore, the MWCNT-modified surface exhibited an increased current response compared to control sensors without MWCNTs. This phenomenon may be attributed to the increased surface area, promoting the increased mass transfer of the analyte.[41] The limit of detection for the P4VP-wrapped MWCNT electrode was calculated to be 0.5 ppm (7.8 μM) by taking 3σ/slope, where σ was the standard deviation of the blank. The calculated limit of detection 0.5 ppm is below the United States EPA limit of 1.3 ppm.

Importantly, an extended cathodic deposition timeframe was not required due to the polymer matrix acting as the preconcentration layer enabling copper detection with lower power compared to sensors that utilize stripping voltammetry. While square wave voltammetry (SWV) is sometimes employed in sensing strategies to decrease the contribution of the charging (i.e., capacitive) current to enhance sensitivity, these methods couple the oxidation and reduction responses of the molecule of interest and may be subject to interference from cathodic oxygen reduction. Thus, CV was chosen as the optimal method due to the clearly resolved oxidation signal at 0.015 V vs Ag/AgCl QRE.

To probe whether the sensor response could be reproduced, calibrated sensors were soaked in a dilute ethylenediaminetetraacetic acid (EDTA) solution for 2−3 h with stirring to remove bound copper. Performing the copper calibration after EDTA treatment, we observed a similar linear response comparable to a freshly made sensor (Figure S15).

Interference studies were carried out in the presence of 20 ppm of Cu^{2+} ions with equal m/v concentrations of potential interfering ions using CV. Typically, 20 ppm Cu^{2+} was chosen to evaluate the effect of interferents based on an optimal CV response at this concentration. Equal concentration with competing metal ions was to further show that Cu^{2+} was preconcentrated selectively to the surface. The CV was done in the presence of interfering ions and again after rinsing with deionized water for approximately 30 s (Figure S16). The spray-printed sensor exhibited selectivity to Cu^{2+} ions over selected interfering ions, including calcium (Ca^{2+}), lead (Pb^{2+}), and iron (Fe^{3+}). These species were chosen based on literature precedent, and a full analysis of interferent effects from both organic and metal species commonly found in environmental matrices on chelating polymer-wrapped MWCNTs will be the subject of future investigations. Copper is preferentially detected over other metal ions as shown by its more pronounced current response after rinsing the electrode with DI water to remove the unbound or loosely bound interfering metal ions. Using the P4VP-wrapped MWCNT electrode, only the Cu^{2+} peak was more pronounced despite equivalent concentrations of Cu^{2+} and Pb^{2+} (Figure 6a). The voltammogram shows that Cu^{2+} is preferentially detected over Pb^{2+} by its stronger signal. Rinsing the electrode with DI water and sweeping the voltage a second time showed a more pronounced Cu^{2+} signal than Pb^{2+}, suggesting Pb^{2+} does not bind to the surface as strongly as Cu^{2+} ions. To further explore the sensor performance, spike tests were performed using synthetic ocean water, creek water from Durden Creek located in Vicksburg, MS, and tap water obtained from Vicksburg, MS. Each sample was spiked with 3 ppm Cu^{+2} and found to give nearly identical responses regardless of the matrix (Figure 6b and Table S2).

Stability testing was performed by carrying out CV periodically for 24 h using three sensors submerged in Cu^{2+} solutions at concentrations that were within the lower linear range of the sensor 1.3, 8.9, and 16.8 ppm (Figure 6c). The three sensors showed a percent relative standard deviation of 7.56, 10.12, and 4.93%, respectively, when monitored at +0.051 V. Future investigations will aim to understand the fundamental nature of these redox responses to further extend the polymer-wrapped MWCNT sensing method.

3. CONCLUSIONS

We have demonstrated the fabrication and application of a polymer-wrapped MWCNT sensor amenable to low-power monitoring of copper in natural waterways. The sensing architecture was extensively examined using Raman spectroscopy, scanning electron microscopy, energy-dispersive spectroscopy, atomic force microscopy, infrared spectroscopy, and contact angle measurements. The electrochemical analysis produced a calibration curve with a linear range of 1.1−13.8 ppm (16.6−216 μM) and a limit of detection of 0.5 ppm (7.8 μM). Hence, this electrochemical sensing platform is suitable for environmental analysis if coupled with a field-portable potentiostat, where rapid on-site monitoring is necessary. While many established methods exist for the quantification of copper in environmental water samples, in this work, we have

https://dx.doi.org/10.1021/acsomega.0c04776
ACS Omega 2021, 6, 5158−5165

demonstrated the feasibility of chelating polymer-wrapped MWCNTs for metal ion detection using Cu^{2+} as a model system. Future studies will focus on optimizing the presented platform and contextualizing it with other established methods. Chelating polymer-wrapped MWCNTs represent a creative means of preconcentrating trace analytes at the electrode surface and may be used in conjunction with low SWaP-C electronic architecture to generate next-generation deployable sensors.

4. MATERIALS AND METHODS

4.1. Apparatus and Reagents. Deionized water (DI water) was obtained from a Millipore Milli Q Advantage DI water system, ethyl alcohol 200 proof (CAS #64-17-5), acetone ≥99.5% ACS reagent (CAS #67-64-1), sulfuric acid 98% (CAS #7664-93-9), (3-aminopropyl)triethoxysilane 99% (CAS #919-30-2), methanol anhydrous, 99.8% (CAS #67-56-1), Triton X100 laboratory grade (CAS #9002-93-1), copper-(II) chloride anhydrous, powder, ≥99.995% trace metal basis (CAS #7447-39-4), copper (II) sulfate pentahydrate (CAS #7758-99-8), (3-bromopropyl)trimethoxysilane ≥97.0% (CAS #51826-90-5), poly(4-vinyl pyridine) average MW ∼160 000 (CAS #25232-41-1), poly(vinyl alcohol) approx. MW ∼160 000 (CAS #25213-24-5), and poly(4-vinylphenol) (CAS #24979-70-2) were purchased from Sigma-Aldrich (St. Louis, MO) and used as received. Carboxyl-functionalized multiwalled carbon nanotubes (MWCNT-COOH) 20−30 nm (SKU: 030304) were obtained from Cheap Tubes Inc. (VT). UV/ozonolysis was performed in UV−Ozone cleaner—ProCleaner plus from BioForce NanoSciences (UT). Fisherbrand Q500 Sonicator with Probe from Fisher Scientific (MA) was used in all ultrasonication processes. Thermo Scientific ST16 Centrifuge (MA) was used for centrifugation. A Nicolet iS 10 FTIR spectrometer with ATR attachment from Thermo Fisher Scientific (MA) was used for Fourier-transform infrared spectroscopy (FTIR) characterizations. Contact angle measurements were obtained through a Drop Shape Analyzer—DSA25 from KRÜSS (NC), SEM imaging and energy-dispersive X-ray (EDX) scans were done using a Phenom Pharos Desktop SEM from Thermo Fisher Scientific (MA), and a Dimension XR atomic force microscope (AFM) from Bruker (CA) was used for surface analysis. Raman spectroscopy was achieved by DXR3 Raman microscope from Thermo Fisher (MA). UV−vis spectroscopy was conducted using a Thermo Scientific Evolution 300 UV−vis spectrophotometer. All electrochemical studies were performed using a multichannel *PalmSens4* -Bluetooth-enabled electrochemical station from BASI (IN).

4.2. Pretreatments for Gold Thin-Film Electrodes. All electrodes were washed with DI water followed with ethanol and acetone. The electrodes were then submerged in 0.05 M H_2SO_4 acid and subjected to electrochemical conditioning, where cyclic voltammetry (CV) was performed in the potential range of 0.2−1.5 V using previously reported methodology[42] until a stable current signal was obtained (approximately 5−8 cycles). The electrodes were rinsed with DI water several times and transferred to a closed vessel purged with nitrogen for 24 h to remove any surface-bound oxygen.

4.3. Functionalization of the PET-Based Gold Electrode Surface. The pretreated sensors were placed in the UV/Ozone chamber for 2 h. 3% v/v (3-aminopropyl)-triethoxysilane (APTES) was selected to mediate MWCNT attachment through hydrogen bonding, and 3% (3-bromopropyl)trimethoxysilane (BPTMS) was used to anchor the incoming MWCNT polymer dispersion via covalent bonding. These reactions are a combination of four steps to achieve hydrolytic deposition of silanes.[43,44] The first step was hydrolysis of the ethoxy groups in APTES via 95% ethanol. Next, the PET-carboxyl/hydroxyl surface was introduced into this solution and kept at room temperature for 48 h. This accommodates the hydrolysis reaction prior to the formation of hydrogen bonds. Afterward, PET films were thoroughly washed with ethanol to remove unbound APTES. The film was then exposed to 50 °C heated surfaces to enhance bond formation between the APTES and the PET substrate. Afterward, they were stored in a humidity-controlled (33.0% RH) storage box until further use.

4.4. Preparation of Carbon Nanotube (CNT)-Based Dispersion. The procedure was performed according to previously reported literature with necessary modifications.[45] First, 20 mg of MWCNT-COOH was transferred into a falcon tube, and 40 mL of methanol was added with three drops of Triton X100 to enhance dispersion of the MWCNTs[46,47] and ultrasonicated in an ice bath for 15 min. Next, 200 mg of poly-4-vinyl pyridine (P4VP) was added into the solution and further ultrasonicated (using a probe-tip sonicator) for 30 min in an ice bath. This solution was centrifuged at 6800 rpm for 30 min to remove undispersed CNTs. The resulting pellet was discarded, and the supernatant was stored at 4 °C. Additional details of all of the other methods used in this work can be found in the Supporting Information (Pages S3−S13).

■ ASSOCIATED CONTENT

Supporting Information

The Supporting Information is available free of charge at https://pubs.acs.org/doi/10.1021/acsomega.0c04776.

Complete experimental details, compound characterization, method of fabrication, related spectra, contact angle measurements, ICP-MS data, electrochemical methods, SEM imaging, related additional CVs, and other related electrochemical measurements (PDF)

■ AUTHOR INFORMATION

Corresponding Author

Gilbert K. Kosgei − *Environmental Laboratory, US Army Engineer Research and Development Center, Vicksburg, Mississippi 39180, United States;* orcid.org/0000-0002-4924-0246; Email: Gilbert.K.Kosgei@usace.army.mil

Authors

P. U. Ashvin Iresh Fernando − *Benton Aerospace, Cary, North Carolina 27518, United States*

Erik Alberts − *Simetri, Inc., Winter Park, Florida 32792, United States;* orcid.org/0000-0001-7230-6744

Matthew W. Glasscott − *Oak Ridge Institute for Science and Education, Oak Ridge, Tennessee 37831, United States; Department of Chemistry, The University of North Carolina at Chapel Hill, Chapel Hill, North Carolina 27599, United States;* orcid.org/0000-0001-5743-7738

Anton Netchaev − *Information Technology Laboratory, US Army Engineer Research and Development Center, Vicksburg, Mississippi 39180, United States*

Jason D. Ray − *Information Technology Laboratory, US Army Engineer Research and Development Center, Vicksburg, Mississippi 39180, United States*

https://dx.doi.org/10.1021/acsomega.0c04776
ACS Omega 2021, 6, 5158−5165

Keith Conley − *Information Technology Laboratory, US Army Engineer Research and Development Center, Vicksburg, Mississippi 39180, United States*
Rishi Patel − *Jordan Valley Innovation Center, Missouri State University, Springfield, Missouri 65806, United States*
Jonathan Fury − *Jordan Valley Innovation Center, Brewer Science, Inc., Springfield, Missouri 65804, United States*
David Henderson − *Environmental Laboratory, US Army Engineer Research and Development Center, Vicksburg, Mississippi 39180, United States*
Lee C. Moores − *Environmental Laboratory, US Army Engineer Research and Development Center, Vicksburg, Mississippi 39180, United States*

Complete contact information is available at: https://pubs.acs.org/10.1021/acsomega.0c04776

Author Contributions

P.U.A.I.F. and G.K.K. are considered as equally contributing first authors of this manuscript. P.U.A.I.F. and G.K.K. designed and performed the experiments and analyzed the data. E.A. performed the surface characterizations and contributed to preparing the manuscript. M.W.G. helped in analysis of electrochemistry based experiments and editing of the manuscript. A.N., J.D.R., and K.C. helped in electrochemical measurements. D.H. helped with the automated spray painter. R.P. and J.F. helped in fabricating the electrode system onto the PET surface. L.C.M. supervised all aspects of this project. All authors collectively have agreed to the final version of this manuscript.

Funding

This work was made possible under Project Number 489630 and Contract W912HZ1820003 through the United States Army Corps of Engineers, Engineer Research and Development Center, Installations and Operational Environment Program (USACE-ERDC-IOE).

Notes

The authors declare no competing financial interest.

■ ACKNOWLEDGMENTS

The use of trade, product, or firm names in this report is for descriptive purposes only and does not imply endorsement by the U.S. Government. The tests described and the resulting data presented herein were obtained from research conducted under the Environmental Quality and Technology Program of the United States Army Corps of Engineers by the USAERDC (WIC 02L0D5). Permission was granted by the Chief of Engineers to publish this information. The findings of this report are not to be construed as an official Department of the Army position unless so designated by other authorized documents. The authors also thank Dr. Rebecca Crouch and Dr. Bobbi Stromer for their review of this document.

■ REFERENCES

(1) Malachová, K.; Praus, P.; Rybková, Z.; Kozák, O. Antibacterial and Antifungal Activities of Silver, Copper and Zinc Montmorillonites. *Appl. Clay Sci.* **2011**, *53*, 642−645.
(2) Barceloux, D. G.; Barceloux, D. Copper. *Clin. Toxicol.: Clin. Toxicol.* **1999**, *37*, 217−230.
(3) Davis, J. R. Copper and Copper Alloys. In *ASM Specialty Handbook*; ASM International: Materials Park, Ohio, 2001.
(4) National Research Council (US) Committe on Copper in Drinking Water. *Health Effects of Excess Copper*; 2000.
(5) United States Environmental Protection Agency. *Lead and Copper Rule: A Quick Reference Guide*; 2008.
(6) Chung, C. Y.; Posimo, J. M.; Lee, S.; Tsang, T.; Davis, J. M.; Brady, D. C.; Chang, C. J. Activity-Based Ratiometric FRET Probe Reveals Oncogene-Driven Changes in Labile Copper Pools Induced by Altered Glutathione Metabolism. *Proc. Natl. Acad. Sci. U.S.A.* **2019**, *116*, 18285−18294.
(7) He, W.; Liu, Z. A Fluorescent Sensor for Cu^{2+} and Fe^{3+} Based on Multiple Mechanisms. *RSC Adv.* **2016**, *6*, 59073−59080.
(8) Wang, M.; Ma, D.; et al. A Colorimetric Chemosensor for Cu^{2+} Ion Based on an Iridium (III) Complex. *Sci. Rep.* **2014**, *3*, No. 6794.
(9) Li, Y.; Tong, J.; Bian, C.; Dong, H.; Sun, J.; Xia, S. In *A Portable Sensor System for Determination of Copper Ions in Waters with Android Device*, Proceedings of IEEE Conference; 2019.
(10) Hassan, K. M.; Elhaddad, G. M.; AbdelAzzem, M. Voltammetric Determination of Cadmium(II), Lead(II) and Copper-(II) with a Glassy Carbon Electrode Modified with Silver Nanoparticles Deposited on Poly(1,8-Diaminonaphthalene). *Microchim. Acta* **2019**, *186*, No. 440.
(11) Borrill, A. J.; Reily, N. E.; Macpherson, J. V. Addressing the Practicalities of Anodic Stripping Voltammetry for Heavy Metal Detection: A Tutorial Review. *Analyst* **2019**, *144*, 6834−6849.
(12) Yang, W.; Wang, Y.; Yang, X.; et al. Polymer Wrapping Technique: An Effective Route to Prepare Pt Nanoflower/Carbon Nanotube Hybrids and Application in Oxygen Reduction. *Energy Environ. Sci.* **2010**, *3*, 144−149.
(13) Schroeder, V.; Savagatrup, S.; He, M.; Lin, S.; Swager, T. M. Carbon Nanotube Chemical Sensors. *Chem. Rev.* **2019**, *119*, 599−663.
(14) Schnorr, J. M.; Swager, T. M. Emerging Applications of Carbon Nanotubes. *Chem. Mater.* **2011**, *23*, 646−657.
(15) do Amaral Montanheiro, T. L.; Cristóvan, F. H.; Lemes, A. P.; et al. Effect of MWCNT Functionalization on Thermal and Electrical Properties of PHBV/MWCNT Nanocomposites. *J. Mater. Res.* **2015**, *30*, 55−65.
(16) Star, A.; Stoddart, J. F.; Steuerman, D.; Diehl, M.; Boukai, A.; Wong, E. W.; Yang, X.; Chung, S.; Choi, H.; Heath, J. R. Preparation and Properties of Polymer- Wrapped Single-Walled Carbon Nanotubes. *Angew. Chem., Int. Ed.* **2001**, *40*, 1721−1725.
(17) Gotoh, K.; Yasukawa, A.; Kobayashi, Y. Wettability Characteristics of Poly (Ethylene Terephthalate) Films Treated by Atmospheric Pressure Plasma and Ultraviolet Excimer Light. *Polym. J.* **2011**, *43*, 545−551.
(18) Hah, J.; Song, B.; Moon, K. J.; Graham, S.; Wong, C. P. In *Design and Surface Modification of PET Substrates Using UV/Ozone Treatment for Roll-to-Roll Processed Solar Photovoltaic (PV) Module Packaging*, IEEE 68th Electronic Components and Technology Conference, 2018; pp 2397−2403.
(19) Tamai, T.; Watanabe, M.; Mitamura, K. Modification of PEN and PET Film Surfaces by Plasma Treatment and Layer-by-Layer Assembly of Polyelectrolyte Multilayer Thin Films. *Colloid Polym. Sci.* **2015**, *293*, 1349−1356.
(20) Fattahi, F. S.; Izadan, H.; Khoddami, A. Investigation into the Effect of UV/Ozone Irradiation on Dyeing Behaviour of Poly(Lactic Acid) and Poly(Ethylene Terephthalate) Substrates. *Prog. Color, Color. Coat.* **2012**, *5*, 15−22.
(21) Ton-That, C.; Campbell, P. A.; Bradley, R. H.; et al. Surface Characterisation of Ultraviolet-Ozone Treated PET Using Atomic Force Microscopy and X-Ray Photoelectron Spectroscopy. *Surf. Sci.* **1999**, *433*−*435*, 278−282.
(22) King, D. E. Oxidation of Gold by Ultraviolet Light and Ozone at 25 °C. *J. Vac. Sci. Technol., A* **1995**, *13*, 1247−1253.
(23) Linn, J. H.; Swartz, W. E. XPS Study of the Effects of Cf4 Plasmas on Gold Surfaces. *Appl. Spectrosc.* **1985**, *39*, 755−760.
(24) Muthuvijayan, V.; Gu, J.; Lewis, R. S. Analysis of Functionalized Polyethylene Terephthalate with Immobilized NTPDase and Cysteine. *Acta Biomater.* **2009**, *5*, 3382−3393.

(25) Nishide, H.; Deguchi, J.; Tsuchida, E. Complex Formation of Crosslinked Poly(4-Vinylpyridine) Resins with Copper(II). *Bull. Chem. Soc. Jpn.* **1976**, *49*, 3498−3501.
(26) Syukri, S.; Hijazi, A. K.; Sakthivel, A.; Al-Hmaideen, A. I.; Kühn, F. E. Heterogenization of Solvent-Ligated Copper(II) Complexes on Poly(4-Vinylpyridine) for the Catalytic Cyclopropanation of Olefins. *Inorg. Chim. Acta* **2007**, *360*, 197−202.
(27) Ottaviani, M. F. An ESR Study on the Interaction of Copper (II) with Pyridine and Poly(2-Vinylpyridine) in Ethanol Solutions. *Colloids Surf.* **1984**, *12*, 305−318.
(28) Hua, J.; Wang, Z.; Zhao, J.; Xu, L.; Zhang, J. I.; Li, R.; Sun, X. A Simple and Facile Approach to Synthesize Water-Soluble Multiwalled Carbon Nanotubes Wrapped by Poly(4-Vinylpyridine). *J. Macromol. Sci., Part B* **2011**, *50*, 679−687.
(29) Fujigaya, T.; Nakashima, N. Non-Covalent Polymer Wrapping of Carbon Nanotubes and the Role of Wrapped Polymers as Functional Dispersants. *Sci. Technol. Adv. Mater.* **2015**, *16*, No. 024802.
(30) den Hoed, F.; Pucci, A.; Picchioni, F.; Raffa, P. Design of a pH-Responsive Conductive Nanocomposite Based on MWCNTs Stabilized in Water by Amphiphilic Block Copolymers. *Nanomaterials* **2019**, *9*, No. 1410.
(31) Noguchi, Y.; Fujigaya, T.; Niidome, Y.; Nakashima, N. Single-Walled Carbon Nanotubes/DNA Hybrids in Water Are Highly Stable. *Chem. Phys. Lett.* **2008**, *455*, 249−251.
(32) Benda, R.; et al. Insights into the $\pi - \pi$ Interaction Driven Non-Covalent Functionalization of Carbon Nanotubes of Various Diameters by Conjugated Fluorene and Carbazole Copolymers Insights into the π−π Interaction Driven Non-Covalent Functionalization of Carbon Nanotube. *J. Chem. Phys.* **2020**, *152*, No. 064708.
(33) Jeon, I.; Chang, D. W. Functionalization of Carbon Nanotubes. In *Carbon Nantubes−Polymer Nanocomposites*; Intech Open Science, 1991.
(34) Nasouri, K.; Shoushtari, A. M.; Mojtahedi, M. R. M. Synthesis and Characterization of Highly Dispersed Multi-Walled Carbon Nanotubes/Polyvinylpyrrolidone Composite Nanofibers for EMI Shielding Application. *Polym. Compos.* **2017**, *38*, 2026−2034.
(35) Hennrich, F.; Krupke, R.; Arnold, K.; Stu, J. A. R.; Lebedkin, S.; Koch, T.; Schimmel, T.; Kappes, M. M. The Mechanism of Cavitation-Induced Scission of Single-Walled Carbon Nanotubes. *J. Phys. Chem. B* **2007**, *111*, 1932−1937.
(36) Bokobza, L.; Zhang, J. Raman Spectroscopic Characterization of Multiwall Carbon Nanotubes and of Composites. *eXPRESS Polym. Lett.* **2012**, *6*, 601−608.
(37) Arrigo, R.; Teresi, R.; Gambarotti, C.; Parisi, F.; Id, G. L.; Dintcheva, N. T. Sonication-Induced Modification of Carbon Nanotubes: Effect on the Rheological and Thermo-Oxidative Behaviour of Polymer-Based Nanocomposites. *Materials* **2018**, *11*, No. 383.
(38) Kishore, S. C.; Pandurangan, A. Fabrication of Solution Processed Carbon Nanotube Embedded Polyvinyl Alcohol Composite Film for Non-Volatile Memory Device. *J. Nanosci. Nanotechnol.* **2014**, *14*, 2381−2387.
(39) Giulianini, M.; Waclawik, E. R.; Bell, J. M.; Scarselli, M.; Castrucci, P.; Crescenzi, M. De.; Motta, N. Microscopic and Spectroscopic Investigation of Poly(3-Hexylthiophene) Interaction with Carbon Nanotubes. *Polymers* **2011**, *3*, No. 1433.
(40) Skoog, M. T.; Jencks, W. P. Reactions of Pyridines and Primary Amines with N-Phosphorylated Pyridines. *J. Am. Chem. Soc.* **1984**, *106*, 7597−7606.
(41) Zhang, S.; Wang, Y.; Han, X.; Cai, Y.; Xu, S. Optimizing the Fabrication of Carbon Nanotube Electrode for Effective Capacitive Deionization via Electrophoretic Deposition Strategy. *Prog. Nat. Sci.: Mater. Int.* **2018**, *28*, 251−257.
(42) Fischer, L. M.; Tenje, M.; Heiskanen, A. R.; Masuda, N.; Castillo, J.; Bentien, A.; Émneus, J.; Jakobsen, M. H.; Boisen, A. Gold Cleaning Methods for Electrochemical Detection Applications. *Microelectron. Eng.* **2009**, *86*, 1282−1285.
(43) Honarvarfard, E.; Gamella, M.; Guz, N.; Katz, E. Electrochemically-Controlled DNA Release under Physiological Conditions from a Monolayer-Modified Electrode. *Electroanalysis* **2017**, *29*, 324−329.
(44) Arkles, B. Tailoring Surfaces with Silanes. *ChemTech* **1977**, *7*, 766−777.
(45) Yoon, B.; Liu, S. F.; Swager, T. M. Surface-Anchored Poly(4-Vinylpyridine)−Single-Walled Carbon Nanotube−Metal Composites for Gas Detection. *Chem. Mater.* **2016**, *28*, 5916−5924.
(46) Keinänen, P.; Siljander, S.; Koivula, M.; Sethi, J.; Sarlin, E.; Vuorinen, J.; Kanerva, M. Optimized Dispersion Quality of Aqueous Carbon Nanotube Colloids as a Function of Sonochemical Yield and Surfactant/CNT Ratio. *Heliyon* **2018**, *4*, No. e00787.
(47) Saran, N.; Parikh, K.; Suh, D. S.; Muñoz, E.; Kolla, H.; Manohar, S. K. Fabrication and Characterization of Thin Films of Single-Walled Carbon Nanotube Bundles on Flexible Plastic Substrates. *J. Am. Chem. Soc.* **2004**, *126*, 4462−4463.

https://dx.doi.org/10.1021/acsomega.0c04776
ACS Omega 2021, 6, 5158−5165